Ultraviolet Microbeam Irradiations of Mitotic Diatoms: Investigation of Spindle Elongation

ROGER J. LESLIE and JEREMY D. PICKETT-HEAPS*
*Biology Department, University of Oregon, Eugene, Oregon 97403; and * Molecular, Cellular, and Developmental Biology, University of Colorado, Boulder, Colorado 80309*

ABSTRACT Our simple instrumentation for generating a UV-microbeam is described. UV-microbeam irradiations of the central spindle in the pennate diatom *Hantzschia amphioxys* have been examined through correlated birefringence light microscopy and TEM. A precise correlation between the region of reduced birefringence and the UV-induced lesion in the microtubules (MTs) of the central spindle is demonstrated. The UV beam appears to dissociate MTs, as MT fragments were rarely encountered.

The forces associated with metaphase and anaphase spindles have been studied via localized UV-microbeam irradiation of the central spindle. These spindles were found to be subjected to compressional forces, presumably exerted by stretched or contracting chromosomes. Comparisons are made with the results of other writers. These compressional forces caused the poles of a severed anaphase spindle to move toward each other and the center of the cell. As these poles moved centrally, the larger of the two postirradiational central spindle remnants elongated with a concomitant decrease in the length of the overlap. Metaphase spindles, in contrast, did not elongate nor lose their overlap region. Our interpretation is that the force for anaphase spindle elongation in *Hantzschia* is generated between half-spindles in the region of MT overlap.

Anaphase separation of chromosomes has long been known to be a two-stage process (specifically in diatoms: see references 20, 28). Inoué and Ritter (16) have recently named the stages "anaphase A" (chromosome-to-pole movement) and "anaphase B" (spindle elongation). Early work in this area has been reviewed by Schrader (43) and Mazia (30). Schrader (43) identified Druner (7) as the first to propose a model of mitosis which includes these two stages. Ris (40) was able experimentally to distinguish between the two stages with chloral hydrate, which inhibits spindle elongation but not chromosome-to-pole movement.

Most models of anaphase spindle elongation agree that interpolar fibers, composed of microtubules (MTs), form a stiff framework that grows and pushes the poles apart, but the models differ in how the elongation is accomplished. Manton et al. (28), working with the centric diatom *Lithodesmium*, suggested that central spindle elongated by growth of MTs at the pole, an interpretation echoed by Brinkley and Cartwright (6) for mitosis in cultured PtK_1 cells and Chinese hamster fibroblasts. Inoué and Sato (14) envisaged a model in which MTs in a dynamic equilibrium with their subunits can move chromosomes via length changes. They proposed that MTs are disassembled primarily at the poles. It is known that MTs grow during anaphase spindle elongation in some cell types, for example in *Diatoma* (22), *Ochromonas* (50), and *Barbulanympha* (16). It is, however, not clear that this MT assembly is always involved in anaphase spindle elongation.

McIntosh et al. (24) and Margolis et al. (29) proposed that sliding of antiparallel MTs in the interzone pushes half-spindles apart, while Pickett-Heaps et al. (34) suggest that sliding of two half-spindles accommodates spindle elongation in the diatom *Diatoma*. By comparing MT counts in the interzone of spindles of cells from two tissue types in the chick embryo, Allenspach and Roth (2) functionally implicated interzonal MTs in elongation. On the other hand, when viewed in the polarization microscope the interzone at anaphase in some cells appears isotropic (42, 47), suggesting that elongation can occur without interzonal MTs. Mazia (30; see Fig. 69 *D* therein) points out that birefringent fibers definitely pass through some interzones that otherwise appear isotropic. Since birefringence depends on organization and orientation of MTs, experimentally observed isotropism does not necessarily prove the absence of MTs.

Models which do not involve the interpolar MTs in spindle

THE JOURNAL OF CELL BIOLOGY · VOLUME 96 FEBRUARY 1983 548-561

elongation have also been proposed. Belar (4, 5) suggested that as the interzone grew it pushed the anaphase chromosomes poleward. Aist and Berns (1) demonstrated that the poles of a telophase spindle in the fungus *Fusarium* separate faster after the central spindle has been severed. Their model involves astral MTs in pulling the poles apart. Regardless of the mechanism of spindle elongation, it is important that the poles are held apart during anaphase chromosome movement; otherwise they would likely move towards the chromosomes. For example, following UV-irradiation of the cytoplasm of cultured newt cells (52), centrosomes moved centrally after the spindle was destroyed.

In 1965, Stephens (45), using a UV-microbeam, was able to distinguish between several hypotheses of the mechanism of striated muscle contraction and supported the now generally accepted sliding filament model. The diatom spindle is another highly organized motile system in which fibers appear to slide relative to each other. This paper describes microbeam irradiations of anaphase diatom spindles which shed some light on the mechanism of spindle elongation. In addition, the experiments give information about the direction and location of forces acting on both metaphase and anaphase spindles.

MATERIALS AND METHODS

The pennate diatom *Hantzschia amphioxys* was collected from the wild near Eugene, Oregon. Cells varied widely in length (150–270 μm) but not in width (30–35 μm) when observed in girdle view. They were cultured as previously described (37). Light and electron microscopy of normal mitosis in *Hantzschia* has been described elsewhere (37, 38). Fluorescent illumination (200 foot-candles) was on a 15/9 h:light/dark cycle. Mitotic divisions were most numerous during the 4–5 h following the start of the dark cycle. Cells were immobilized for irradiations by sandwiching them between a thin agar pad (1% agar made up in culture medium, on a mounting cover slip) and the quartz cover slip (from Bond Optics, 22 mm^2). The appendix describes our equipment and experimental procedures.

Measurements of the spindle, both from slides and from the recorded image on the TV monitor, were taken by placing a sheet of acetate on the monitor screen and marking the positions of spindle features with a Sharpie pen. A new sheet of acetate was used for each set of points. The measurements taken in this way for Fig. 9 were confirmed by taking 35mm slides of the monitor screen at consecutive times spaced 15 s apart. These slides were projected to × 15,000, and the positions of spindle structures were marked with a pencil.

A diagram of the irradiation slit is presented in some figures; a photographic image in others. This is a consequence of changes in the polarization image of the spindle when the dichroic mirror is moved into the path of the field illumination. The dichroic mirror shifts the plane polarized field illumination and the polarization cross observed in the back focal plane of the objective, a small distance perpendicular to the optical axis of the microscope, thus changing the contrast of the image of the spindle. Optimal spindle contrast can be re-established by adjusting the compensator; however, this was not generally done because it was then difficult to compare the birefringence of the spindle before and after irradiation when the dichroic mirror was no longer in the light path. After many experiments had been completed, it became apparent that there was little or no change in the overall birefringence of the spindle after irradiation, and so photographs of the visible image of the irradiation aperture were taken. It is also true that the visible image of the irradiation aperture is no guarantee, anyway, of the position of the focused UV beam which is best indicated by the effect (lesions) produced by that beam on the MTs of the central spindle.

172 irradiations were recorded with the TV system, and another approximately 100 irradiations were observed prior to the availability of this recording equipment. 80 cells were fixed and 20 sectioned for electron microscope examination. Electron micrographs of all serial sections through the spindle were obtained in eight cases.

RESULTS

Controls

The irradiation beam was heterochromatic and it was necessary to estimate the effects of visible and infrared wavelengths on the spindle. This control was accomplished by placing a glass cover slip in the microbeam irradiation path. The glass cover slip (#1.5) is virtually opaque to UV wavelengths below 300 nm and transparent to light >320 nm. The subsequent cell division in cells irradiated with the UV blocked by such a cover slip proceeded normally (Fig. 1). A UV transmission filter (λ_{max} = 273 nm) was not used in the irradiation path, because of the 60–90-s-irradiation time that then became necessary with the attenuated beam. Test irradiations through this filter did produce a loss of birefringence in the central spindle, but over the final 3–5 s of these long irradiations. This slower loss of birefringence created less distinct lesion edges. While the behavior of spindles irradiated with this filtered light was entirely similar to that of cells irradiated without the filter, the longer exposure time permitted many of the lesion's effects to be less well defined.

Irradiations of the duration used to produce the lesions described below, when directed instead outside of the central spindle (including the area adjacent to the spindle poles), did not produce abnormal divisions, excepting irradiations which included the narrow band of Golgi bodies and mitochondria surrounding the nucleus. When this membrane band was irradiated the birefringence of the spindle was reduced. This procedure does not represent a particularly useful control to investigate possible nonspecific effects generated by the irradiation, because the cytoplasm surrounding the spindle is quite different from that in the spindle and, consequently, irradiations of the two different areas might have different results.

The birefringent keratin fibers of buccal epithelial cells and the edge of the ingrowing cleavage furrow of *Hantzschia* were irradiated to investigate the sort of differences in UV susceptibility that might be encountered in different cellular structures. Irradiation dosages 10 times greater than those which destroyed microtubules (MTs) in the central spindle produced no lesion in keratin fibers. The cleavage furrow of *Hantzschia* could be stopped with twice the MT-lesional dosage. Interestingly, in these experiments, the irradiated edge of the cleavage furrow was arrested while the companion, unirradiated edge continued to move inwards, stopping at its normal final position in the center of the cell.

Behavior of Spindles after Irradiation: Metaphase

A 3 × 4 μm irradiation of the overlap at the side of the central spindle resulted in rapid (within one minute) bowing of the unirradiated portion of the spindle (Fig. 2), the MTs on either side of the lesion becoming bent toward the center. After the bowing was complete, the cut MTs (R. Leslie and J. D. Pickett-Heaps, manuscript in preparation) often splayed away from the center of the spindle but always remained attached to the poles. A smaller (2 × 2 μm), square irradiation in the center of the overlap did not result in any obvious deformation of the spindle.

Central spindle birefringence disappeared completely after a slit irradiation which severed the central spindle at the overlap. Most of these irradiations were directed at late metaphase—early anaphase spindles, and loss of birefringence is presumably the result of MT disassembly. This phenomenon has important implications which will be described and discussed at length in a following publication.

A lesion placed in the half-spindle that severed or nearly severed it resulted in a rapid collapse of both poles towards the equator of the cell (Fig. 3). The smaller of the two central spindle remnants flipped as it moved centrally, while the pole-

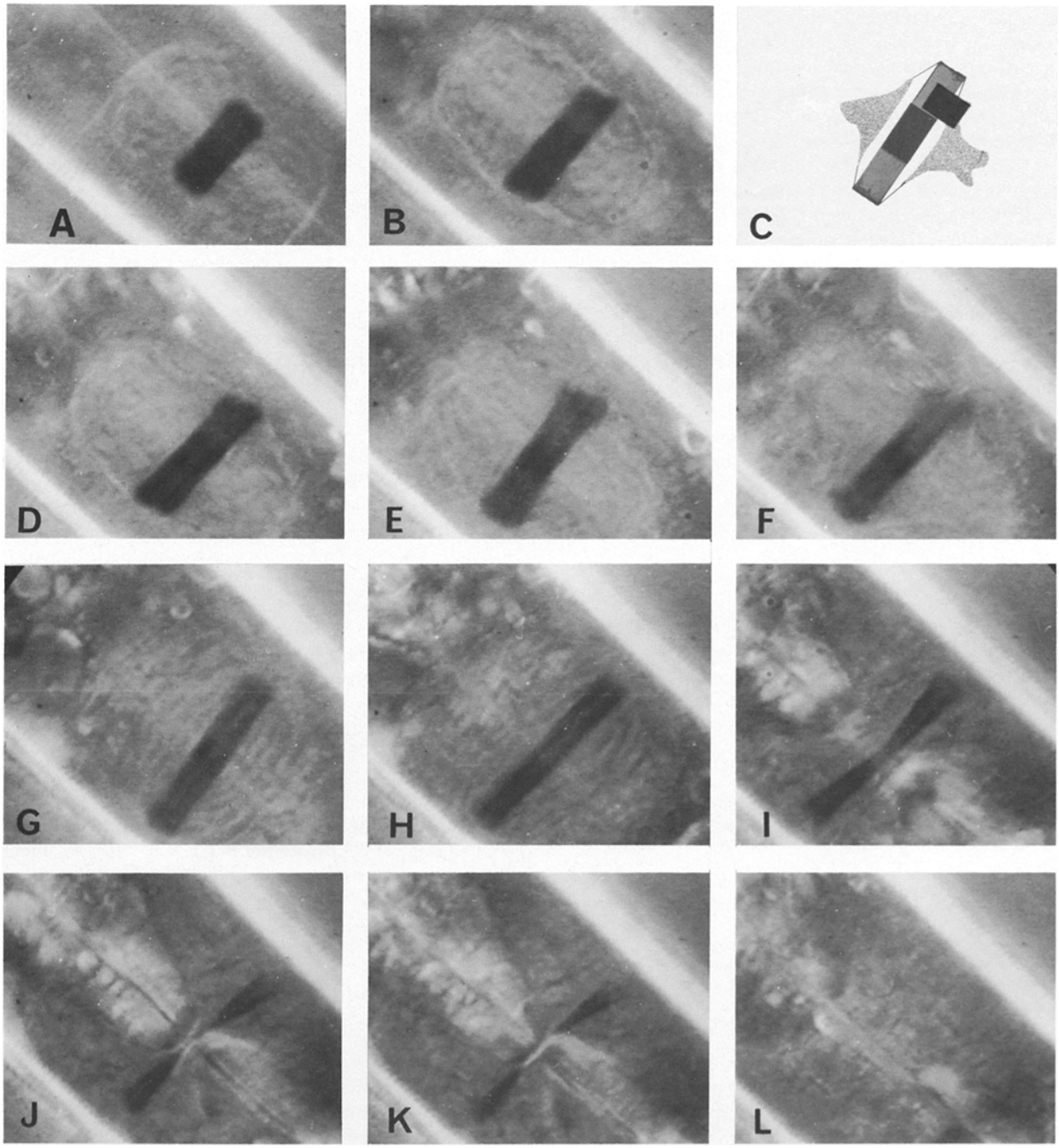

FIGURE 1 Control irradiation; UV light blocked by use of a glass cover slip. Time zero is at the end of the irradiation. (*A*) −4:11. Early prometaphase. Chromosomes are just beginning to associate with the spindle as it sinks into the nucleus. (*B*) −0:57. Mid prometaphase. Most chromosomes are not attached, but kinetochores are quite actively stretching poleward. (*C*) 0:00. Diagram of irradiation. A 3-×-4 μm aperture was focused in the location indicated. A glass cover slip was in the beam path during irradiation. (*D–F*) +0:50, +4:03, and +12:26. Metaphase. Kinetochores attach to poles and the chromosomes are stationary. The overlap appears clearly in the center of the central spindle. The spindle elongates slightly after chromosome attachment. The spindle has rotated out of the plane of focus in *F*. (*G–I*) +20:19, +23:57, and +25:40. Anaphase. Chromosome arms appear and contract around the poles of the central spindle. The overlap decreases in size as the spindle elongates. The spindle constricts in the middle and bends towards the closest vertex of the cleavage furrow. (*J–L*) +26:39, +27:09, and +29:52. Telophase. The cleavage furrow pinches the spindle in the center. The chloroplasts contract towards the cell ends after cleavage. All figures, × 1,500.

to-overlap orientation of the larger remnant did not change (Fig. 4). This collapse was very fast; since we were limited by the mechanical design of our instrument which did not permit viewing of the cell closer than 15 s. from the end of irradiation, we could not follow this collapse in its entirety, unless the spindle was partially severed, in which case there was sometimes a short pause between irradiation and collapse (Fig. 3). The collapsing spindle remnants slowed as the poles approached the center of the chromosome mass (Fig. 5); however, we could not demonstrate a proportionality between the rate of movement and the distance between the equator and the pole.

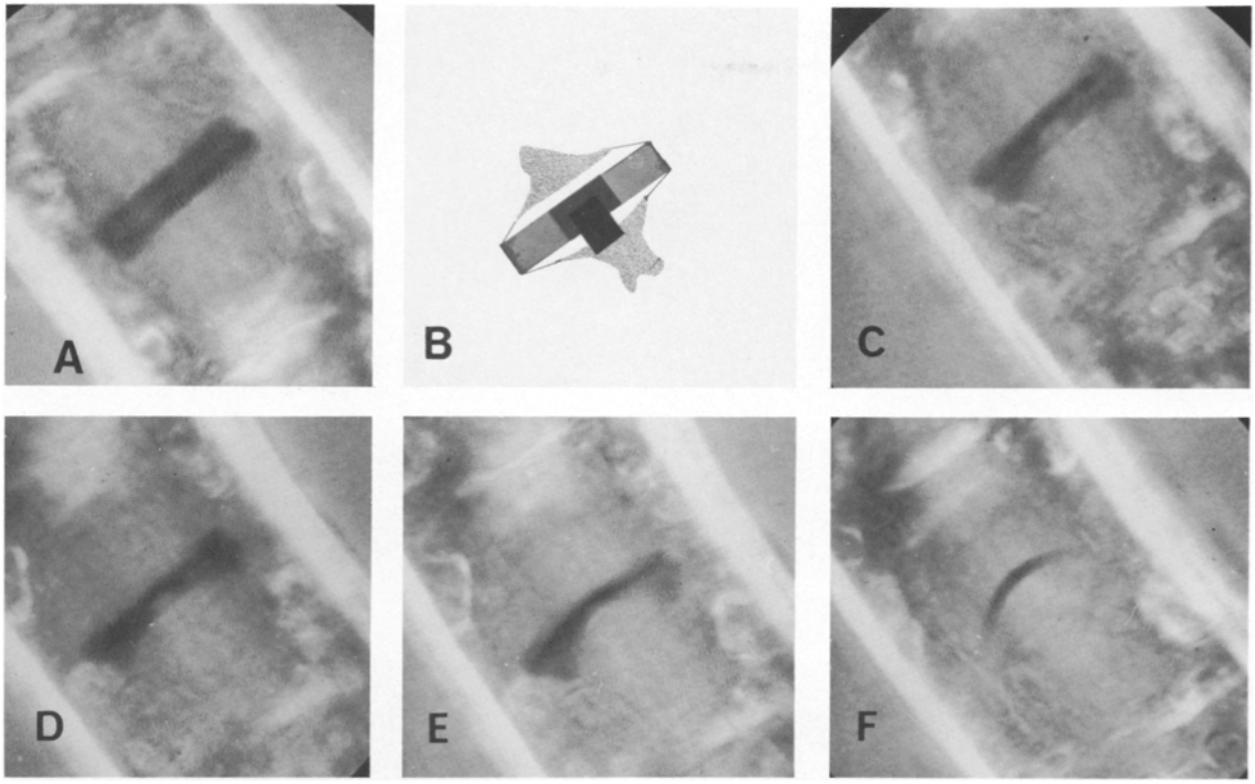

FIGURE 2 Spot lesion in the overlap side of a metaphase spindle. Time zero is the end of the irradiation. (*A*) −0:50. The metaphase cell before irradiation. (*B*) 0:00. A diagram which indicates the approximate relative size and position of the irradiation. (*C*) +0:02. The lesion, immediately after the irradiation, is a clear spot in the black overlap. (*D–F*) +0:05, +0:27, and +1:07. The spindle progressively bows. MTs are still present on either side of the irradiation in *F* but are reduced in birefringence because of suboptimal orientation relative to the axis of polarization. All micrographs, × 2,000.

The stretched chromatin associated with polar MTs, and characteristic of chromosome attachment to the metaphase spindle, was not visible after collapse of the severed central spindle (Fig. 4 *D*). Such chromosomes appeared unable to move, and stretching of kinetochores, characteristic of prometaphase, was never re-established. The overlap never decreased in size while the irradiated cell remained in metaphase (Fig. 4 *D*). A cell could enter an abortive anaphase after an irradiation, whereupon the chromatids appeared to separate and form a stellate array around each pole, both now near the cell equator. During such an anaphase the overlap, still visible in the major portion of the severed central spindle, decreased in length. The other, smaller piece of the spindle was much more difficult to observe because of its highly variable position and its tendency to disassemble (Leslie and Pickett-Heaps, manuscript in preparation). The cleavage furrow passed through the equator of the cell in the position expected after normal anaphase.

The dividing nucleus is enclosed by a layer of Golgi bodies concentrated near the poles. This layer is present during interphase outside the nuclear envelope, and it remains peripheral to the chromosomes as the spindle sinks into the nucleus. In irradiated cells, the Golgi bodies closest to the poles follow them towards the equator of the cell during spindle collapse (Fig. 4 *D*).

Behavior of Spindles after Irradiation: Anaphase

A transverse slit (2 × 8 μm) irradiation across the central region of an anaphase half-spindle severed it. The small polar remnant thus generated disappeared as its birefringence faded polewards from the severed edge (this interesting phenomenon will be described separately by the authors in a manuscript now being prepared). The remaining central spindle portion containing the overlap moved equatorially a small distance. The distance covered seemed to depend on the extent of chromosome arm contraction but it was difficult to quantify contraction accurately enough to produce a meaningful analysis. The movement could be qualitatively recognized by the position that the ingrowing cleavage furrow impinged on the remaining central spindle, outside its overlap. This asymmetric encounter never happens in unirradiated cells. That this movement had occurred was also evident both from spindle position relative to the cell walls and from the displacement of the MT lesion in the central spindle relative to the reduced staining area earlier coincidently generated in the chromosomes (Fig. 6 *G*). This displacement of the two lesions (in the central spindle and chromosomes) was in a direction opposite of that predicted from normal anaphase chromosome movement (Fig. 7). The chromosome masses in these irradiated cells sometimes moved towards each other, accompanying equatorially polar movement, which contributed to the observed relative displacement of the two lesions.

Transverse serial sections were taken of an anaphase cell fixed after a slit irradiation that apparently severed one-half spindle as indicated by the movements of the spindle remnants (Fig. 6). The section of the overlap shown in Fig. 6 *F* contains 1,216 MTs profiles. About three possible MTs profiles, which seemed to be larger than those in Fig. 6 *E* and *F*, were detected in a representative section of the irradiated region, shown in Fig. 6 *J*; clearly, the half spindle had been structurally severed in terms of the integrity of its constituent MTs.

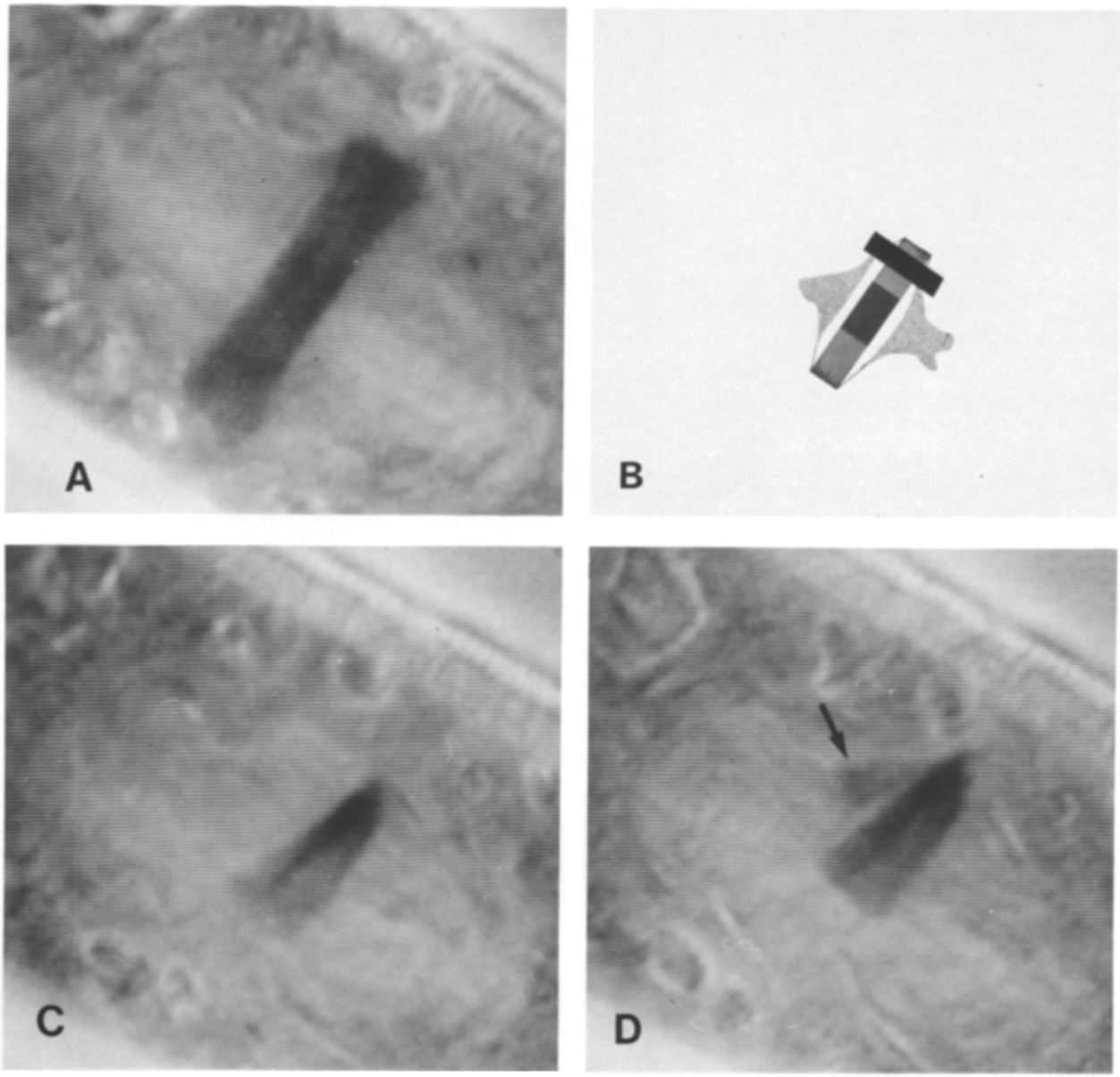

FIGURE 3 A slit irradiation of a metaphase spindle. Time zero is the end of the irradiation. (*A*) −3:06. A metaphase spindle before irradiation. (*B*) 0:00. A diagram of the approximate relative size and position of the slit (2 × 8 μm) irradiation. (*C*) +0:45. The metaphase spindle has been severed. The visible portion of the central spindle includes the overlap and has moved centrally. (*D*) +2:15. An arrow points to the other postirradiation portion of the spindle which has flopped over so that the poles are close to each other. The spindle portion containing the overlap has moved farther towards the center of the chromosome mass. All micrographs, × 3,000.

The major portion of the anaphase central spindle remaining after the severing slit irradiation later elongated with a concomitant loss of its overlap (Fig. 7). This phenomenon was clearest in spindles which elongated before cleavage. When cleavage coincided with elongation, spindle structure changes were more difficult to discern (the relative timing of these two events is somewhat dependent upon the length of cells, quite variable in culture). Fig. 8 is a graphical representation of the behavior of the spindle illustrated in Fig. 9. As in normal cells, the unirradiated half-spindle did not detectably change size during this anaphase elongation; the segment of the severed half-spindle inserted in the overlap was also relatively stable in length, in contrast to the polar segment which rapidly disappeared (Leslie and Pickett-Heaps, manuscript in preparation). The reference point used in Fig. 8, relative to which all spindle movement was measured, was a feature on the wall (one edge of the central gap in the fibulae). In this cell, spindle elongation and movement of the severed spindle were concurrent and, consequently, the pole represented by open squares remained relatively stationary, but the irradiated edge displayed appreciable movement, due to the additive effect here of the two phenomena. Note how the intact half-spindle maintained its length (represented by the distance between the dark circles and the open squares) during its movement.

DISCUSSION

Metaphase Spindle Movement

The most immediate effect of a slit irradiation (i.e., one that traversed the width of the spindle) of a half-spindle at meta-

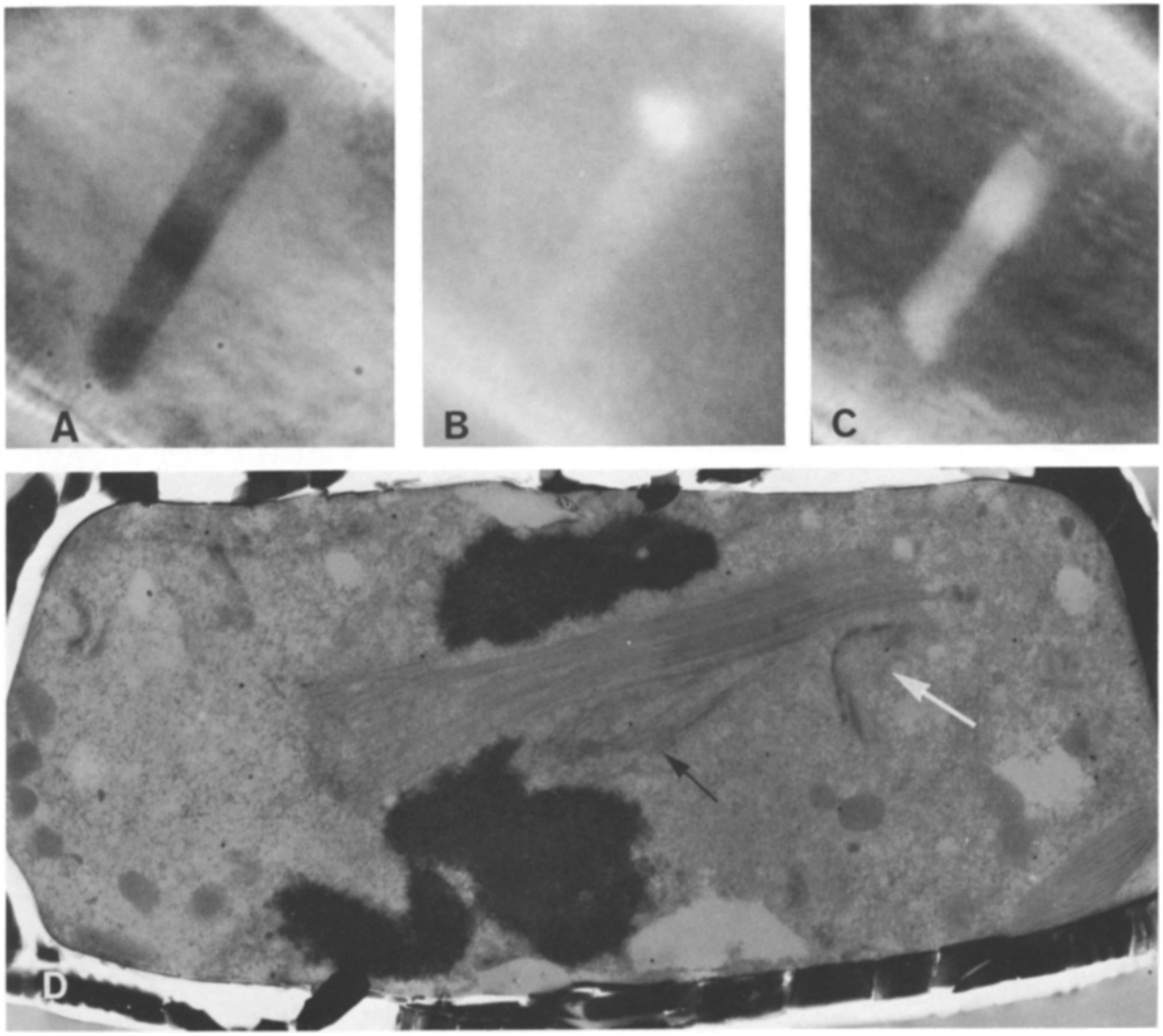

FIGURE 4 Electron micrograph of severed metaphase spindle. Time zero is the end of the irradiation. (*A*) −2:10. The metaphase cell before irradiation. (*B*) −0:20. An image of the visible light portion of the focused aperture. (*C*) +2.35. The severed spindle following fixation. The cell was fixed at 2:33. (*D*) 0.5-μm section taken parallel to the axis of irradiation and photographed in the high voltage electron microscope. The arrow points to a pole which is collapsed centrally. There is no evidence of the stretched kinetochores or kinetochore MTs typical of a normal metaphase. Notice that on the right of the micrograph, just below the lesion edge in the central spindle, there is a densely stained, crescent-shaped plate. This is, presumably, a portion of the polar complex which normally lies adjacent to the pole (white arrow). All light micrographs, × 2,500.

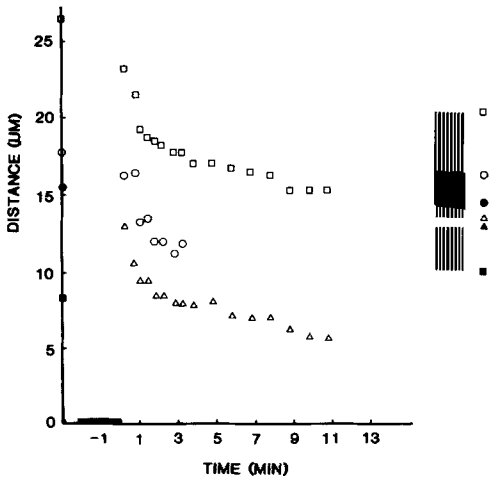

FIGURE 5 Graph of cell in Fig. 3. The reference point for measurements is the cell wall. The positions, relative to this reference point, of the pole are represented by square symbols, the overlap edge by circles, and the lesion edge by triangles. The spindle pole which was separated from the overlap by the irradiation moved in a semicircular pattern (see text) and could not be graphed. The irradiation blackout is represented by a black bar on the abscissa. After irradiation, the spindle portion containing the overlap (between the squares and triangles) moves centrally. The pole of the spindle remnant asymptotically approaches the former position of the center of the overlap (see circles on the ordinate). The edge of the overlap is not distinct enough to measure beyond 3 min after irradiation.

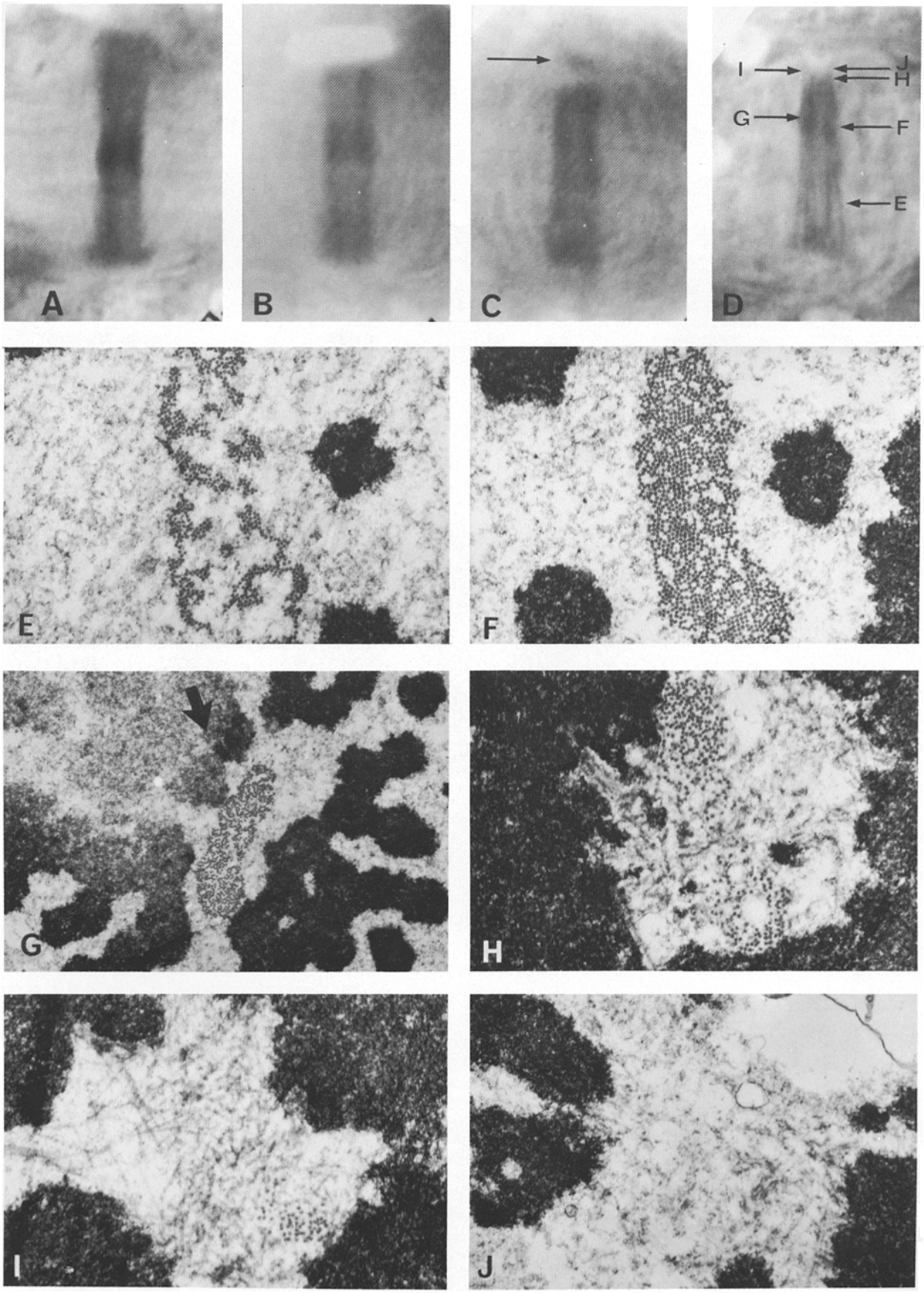
A
B
C
D
I
J
H
G
F
E
E
F
G
H
I
J

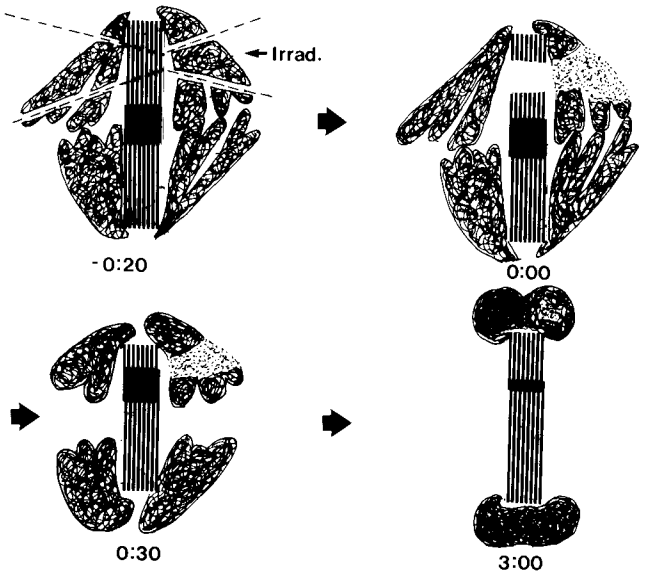

FIGURE 7 Diagrammatic representation of the displacement between damage in chromosomes and the central spindle at anaphase. Time is shown in minutes and seconds. This spindle is viewed along an axis perpendicular to the axis of irradiation. −0:20: Broken lines define the edges of the focused irradiation beam. The focal point is at the surface of the spindle and an arrow (*Irrad.*) points along the axis of wave propagation (away from the irradiation source). 0:00: An area of reduced staining in the chromosomes is coincident with the area of MT disorganization in the central spindle. Chromosomes in the beam path but distal to the irradiation source appear unaffected. +0:30: The postirradiation remnant of the central spindle which does not contain an overlap disappears soon after the irradiation. The overlap-containing remnant moves centrally as the chromosomes continue to contract. The lesion edge of the central spindle remnant and the UV-effect in the chromosomes are displaced relative to each other in a direction opposite that anticipated from chromosome movement alone (Fig. 6). +3:00: The chromosomes contract over the ends of the spindle and the central spindle elongates with a loss of overlap. In Fig. 9, spindle elongation and the postirradiation movement of the central spindle remnant are concomitant.

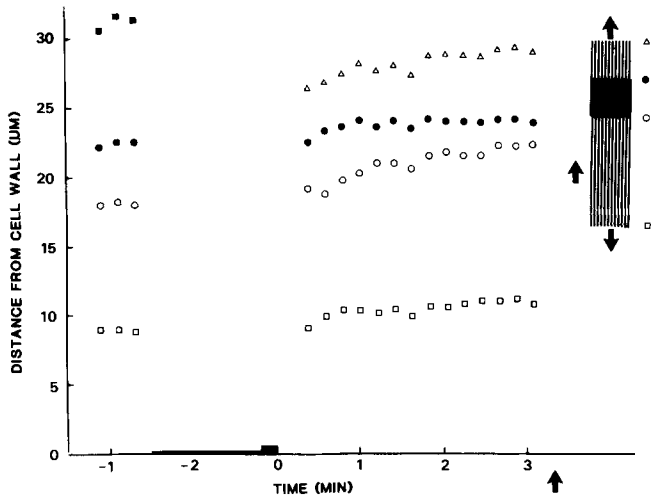

FIGURE 8 Graph showing relative movements of spindle components, from cell in Fig. 9. The thin black bar on the abscissa represents the irradiation blackout period, and the thick bar represents the actual irradiation period. The large arrow on the abscissa points to the time of fixation. The figure symbols are as described in Fig. 3. The diagram at the right illustrates the movement of the half-spindles away from each other and the movement of the entire spindle portion centrally. The stationary reference point was on the cell wall 8.6 μm from the closest edge of the gap in fibulae. The overlap, represented by circles, becomes smaller as the pole (squares) and the lesion edge move apart (triangles). The half-spindle length remains constant.

phase was the rapid collapse of the spindle, with the poles converging centrally. The smaller polar remnant flipped and moved pole-first towards the center of the cell, evidence that the force for such movement is directed at the poles. This behavior is what would be anticipated if the central spindle is under compression generated by the numerous chromatids stretched over it. Basically, the same interpretation can be applied to the observations by Izutsu (17) and by McNeill and Berns (27), in which sister chromatids at metaphase move towards the pole opposite to an irradiated kinetochore. In these cases, the spindle appears under similar tension, but one kinetochore fiber had been cut. Normal diatom spindles also show evidence of this compression, for example, in the bending and bowing of the central spindle MTs in *Pinnularia* (35). The movement of spindle poles towards each other after a slit irradiation of the central spindle equivalent has been observed previously in *Haemanthus* endosperm (13). A similar collapse of centrosomes centrally was observed in cultured newt cells after the spindle was destroyed by irradiation of the cytoplasm (52). Zirkle (52) also described a clustering of chromosomes in a quasirosette with their kinetochores oriented centrally towards the adjacent centrosomes. A similar behavior was observed here but only at the normal onset of anaphase as identified by chromatid separation, MT bundling, and cleavage.

Pickett-Heaps and Tippit (36) have described kinetochore fibers of *Hantzschia* as atypical, although the stretching of the kinetochore region may be quite characteristic of some cell types (12, 32). Kinetochore stretching, quite pronounced in *Hantzschia*, is less dramatic in other diatoms such as *Surirella* and *Pinnularia*. The chromosomes of these diatoms, however,

FIGURE 6 Electron micrographs of a severed anaphase spindle. Time zero is the end of the irradiation. (*A*) −2:04. Metaphase cell before irradiation. Notice the birefringent kinetochore fibers which splay from the poles. (*B*) −0:17. Image of the slit. The cell has begun anaphase. (*C*) +0:12. The irradiation effect. The arrow points to the spindle pole remnant which has already moved centrally. (*D*) +7:04. After fixation, which occurred at +5:56. Arrows point to the positions of transverse sections below. (*E*) 75-nm thin section through the half-spindle. Notice the MTs bundling typical of anaphase spindles. The central spindle located in the center of the densely stained chromosome arms. × 18,000. (*F*) The overlap. This section contains 1,216 MTs profiles. × 18,200. (*G*) Low magnification image showing the overlap and the area of reduced staining typical of chromosome damage. The arrow indicates the approximate axis of irradiation. × 7,500. (*H*) The irradiation edge. × 18,200. (*I*) Two sections beyond *H*. The MTs splay in a polelike fashion. This may be the polar remnant. × 18,200. (*J*) Two sections beyond *I*. A few circular profiles remain but these are larger than the MTs profiles in the other sections. × 14,600. All light micrographs, × 2, 500.

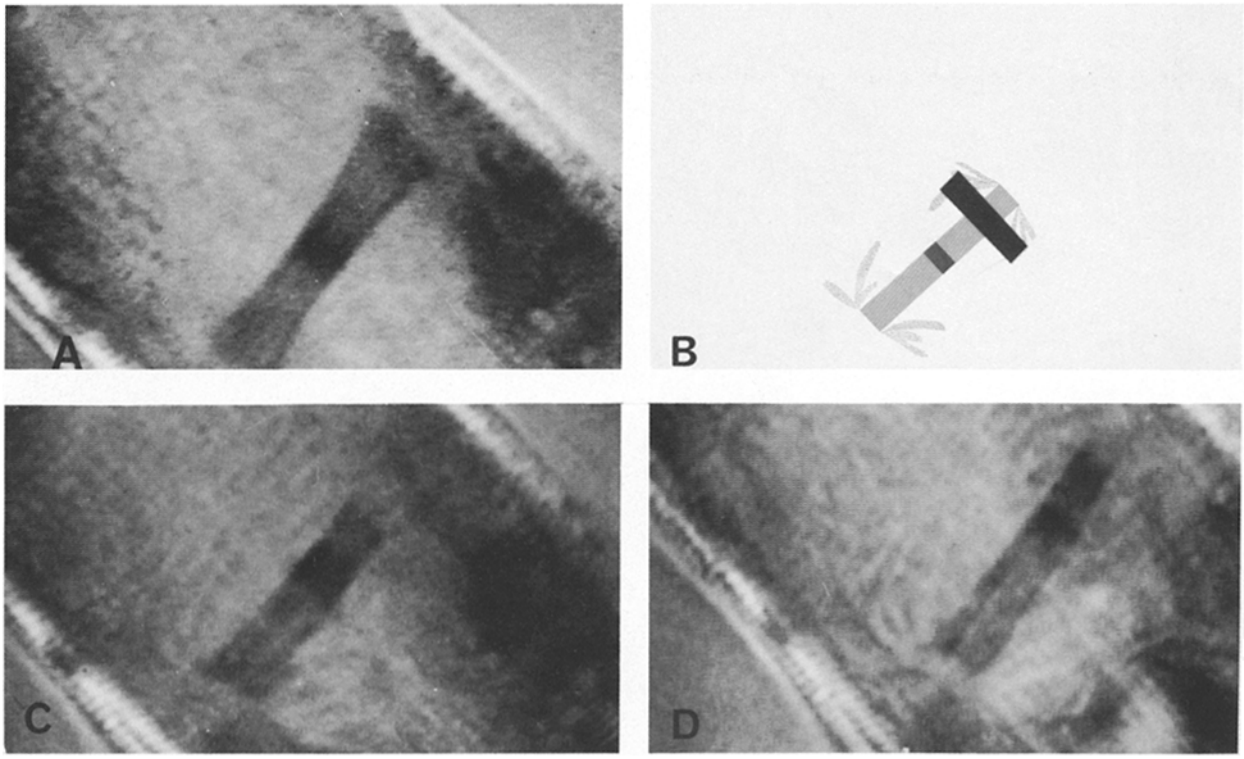

FIGURE 9 Elongation of a severed anaphase spindle. Time zero is the end of the irradiation. (*A*) −2:11. A metaphase cell before irradiation. (*B*) 0:00. A diagram of the relative size and position of the slit (2 × 8 μm) irradiation. (*C*) +0:35. Sister chromatids have separated. The overlap is clearly visible in the remaining portion of the severed central spindle. (*D*) +4:39. The spindle portion has elongated with a concomitant decrease in the size of the overlap. All micrographs are × 3,400.

attach directly to the central spindle and have no identifiable kinetochore fibers (20). More unusual than this kinetochore stretching in *Hantzschia* is the organization of the kinetochore fibers. Almost all MTs of these fibers pass laterally by the plate of the kinetochore and form a cone around the stretched region of the chromosome (49). When the spindle is severed and the poles move toward each other, these MTs ensheathing the kinetochores disappear much more rapidly than the MTs of the smaller central spindle remnant (Leslie and Pickett-Heaps, manuscript in preparation). Our interpretation is that the kinetochore MTs are fragmented against the contracting chromosome mass since MT disassembly (in the small spindle remnant) is much slower than the disappearance of the kinetochore-associated fibers. In the special case of *Hantzschia* it is unlikely that disassembly of MTs of the kinetochore fibers is rate limiting for chromosome movement as proposed for other cell types by Inoué and Ritter (15), Heath and Heath (11), and McNeill and Berns (27).

It is possible that a contractile or elastic component permeates the MTs of the central spindle and is allowed to contract when MTs are locally destroyed. An UV irradiation that removed only the MTs and left the second component intact and functioning would explain the observed inward collapse of the poles. The compressional force on the central spindle by this second component would have to decrease during anaphase.

Anaphase

One of the clearest results of this work is that metaphase spindles when cut transversely do not elongate. Anaphase spindles always do. A severed metaphase spindle may go through the transition to anaphase and elongate. Our interpretation is that this spindle elongation is a discrete process preprogrammed to occur or be activated sometime during anaphase, contrary to the suggestion by Pickett-Heaps and Tippit (36) that spindle elongation is continuous from prophase to telophase interrupted during metaphase by the attachment of chromosomes. This also is contrary to the Margolis et al. (29) model, in which the metaphase spindle is held against sliding of interzonal MTs by the attachment of chromatids. Furthermore, this elongation clearly appears to be generated in the overlap; even when the pole has been removed from a half-spindle, the remnant of that half-spindle later appears to have become extruded from the overlap.

Elongation in normal cells may begin before, during, or after the separation of chromatids at anaphase in *Hantzschia*. A similar generalization was made by Mazia (30) about mitosis in a variety of organisms. The cell in Fig. 1 had begun elongation prior to chromatid separation, with the very small overlap remaining at the beginning of chromatid separation (this cell, a control, reflects a usual course of events). It seems that normal or severed diatom central spindles can elongate in spite of the tendency for the poles and associated components to move towards each other. This conclusion assumes that the equatorial movements of poles after a slit irradiation are manifestations of forces occurring in unirradiated spindles and that they are therefore not artifacts of irradiation. Often (as stated previously), normal diatoms show evidence of such compressional forces in the form of bowed and twisted MTs in the central spindle. Taylor (48) also demonstrated a continuous shortening of the newt spindle during metaphase and suggested that this shortening could be an integral part of the anaphase motion.

It would appear intuitively necessary that a central spindle

or pole-to-pole system of continuous spindle fibers should be present to generate spindle elongation (15, 19, 25, 41). Within the measuring accuracy of light microscopy, half-spindles in *Hantzschia* (and *Pinnularia*: reference 39) remain the same size during anaphase elongation, and so we conclude that half-spindles slide for this elongation. It is also true that MTs comprising the central spindle apparatus almost certainly lengthen by polymerization during anaphase as the spindle elongates in other cells (11, 15, 18, 44, 50, 51) and some diatoms (26, 28). Heath and Heath (11) observed telophase elongation in the fungus *Uromyces* without significant spindle overlap, but they could not exclude the possibility that intertubule sliding coupled with MT polymerization was occurring. Allenspach and Roth (2) compared interzonal MTs in two types of anaphase cells from the chick embryo. Epithelial cells which did not elongate significantly in anaphase did not contain many interzonal MTs; in contrast, mesenchymal cells which underwent extensive anaphase elongation, contained numerous interzonal MTs. These two cell types therefore demonstrated a direct correlation between the presence of interzonal MTs and spindle elongation. While the most likely explanation for anaphase elongation in *Hantzschia* is MTs sliding against antiparallel MTs (22) of the other half-spindle, the MTs could also move against other cytoplasmic components ("swimming"). *Hantzschia's* half-spindles normally do not move farther apart once separated, and so for "swimming" to be a viable explanation of elongation the second component on which the MTs exert their sliding force would have to be confined to the overlap. McDonald et al. (23) hypothesized that the amorphous matrix in the overlap of *Diatoma* could be contractile. Such a contraction could maintain close physical association of antiparallel MTs during sliding. In this regard Leslie (21; Fig. 4) observed a constriction of the overlap in the central spindle in the absence of cleavage.

Aist and Berns (1) have given evidence that spindle elongation can occur without interzonal fibers. They employed a laser microbeam to sever the telophase central spindle of the fungus *Fusarium*, whereupon the poles moved apart at an accelerated rate compared with normal anaphase. They presented a model in which astral MTs pull the poles apart; the central spindle was visualized to limit the rate of pole separation. This mechanism of spindle elongation is not operative in *Hantzschia* but could be in other diatoms (see below).

An overview of diatom spindle elongation suggests that three processes contribute to the separation of chromosomes apart from kinetochore-to-pole movement. These processes are: (*a*) MTs sliding or swimming; (*b*) MT assembly (half-spindle elongation); and (*c*) protoplast contraction. From this viewpoint, MT assembly need not be force producing. *Hantzschia* presumably utilizes MT sliding (or swimming). The MTs of *Diatoma* (22, 23) seem to elongate by polymerization in addition to MT sliding during anaphase. Protoplast contraction has been reported in the centric diatoms *Ditylum* (10) and *Biddulphia* (46) where the contraction occurs after cleavage. Manton et al. (28) working with meiotic divisions in the centric diatom *Lithodesmium* were unable to attribute cell shape changes to spindle elongation alone. (In these three cases, one must also include sliding or swimming.)

Clearly, a variety of mechanisms can contribute to anaphase spindle elongation. Our work here excludes the possibility that astral MTs or cytoplasmic attachments to the poles function in this capacity in *Hantzschia*, contrary to the observations of Aist and Berns (1) in fungi. Simple MT polymerization at the poles is also excluded.

APPENDIX

Used with appropriate living material, the UV-microbeam is a useful experimental tool for investigating cell structure and function. It allows the creation of certain small, well-defined lesions, a form of microsurgery that cannot yet be accomplished any other way than by using a microbeam. It is particularly appropriate for investigating MT-based cellular systems, since MTs appear to be sensitive to localized destruction by UV at the wavelengths used. It is obviously very important to check the ultrastructure of the UV-lesion to confirm the type and extent of damage sustained. In this regard, Bajer (3) found his UV-microbeam of questionable use of dividing *Haemanthus* endosperm, since there was considerable variability in the extent of MT destruction induced, and behavior of the living cell. He considered that the plane of focus of the UV beam appeared critical and difficult to control. Our microbeam, when used with the particularly favorable diatom spindle as the irradiated object, gave excellent and reproducible results over many experiments. We have concentrated on the effects of this microirradiation on MTs and the subsequent behavior of the mitotic spindle. Obviously, however, UV damage is not confined to MTs and chromatin, but we have no information as to how the groundplasm (e.g., components other than MTs in the spindle) could have been effected. Such components may not have any obvious ultrastructural organization even before irradiation; that the ground cytoplasm was indeed affected in irradiated areas was clear from those fixations that were inadvertently stressed during specimen preparation, in which event these areas of cytoplasm invariably suffered gross damage (fracture and breakage) before the remainder of the fixed cytoplasm.

UV APPARATUS: The microbeam apparatus (Fig. 10) was designed around a Zeiss model D inverted microscope. A sliding mount (Fig. 10 *E*) was fabricated which could be inserted in the condenser holder; this slider held a 40X and 100X objective (see below). The speciment was usually observed in polarization optics between two 40X (NA 0.85) Zeiss oil immersion objectives, with the condenser side objective glycerin immersed. For UV-irradiation, a Zeiss 100X (NA 1.25) glycerin-immersion quartz objective was slid across in the place of the 40X objective on the condenser side. The emission of an Osram HBO 200-W AC mercury arc burner (Fig. 10 *A*) was collimated by a Zeiss quartz collector. The source was focused on an aperture (Fig. 10 *C*) which could be adjusted to any rectangular size or shape within the field of the condenser objective. The image of the aperture was reflected into the condenser objective by a dichroic mirror (Fig. 10 *D*) that could be rotated in and out of the optical axis of the microscope. The irradiation aperture was parfocal with the field illumination diaphragm.

A Venus DV-2 two-stage intensified vidicon television camera (Fig. 10 *F*) was used to observe the cells. This sensitive camera allowed visualization of birefringent spindle fibers at relatively low illumination levels. The field illumination source was a 12-V, 100-W quartz halogen bulb (Fig. 10 *B*) generally operated at 6–8 V (as compared to the 200-W mercury arc burner operated at full intensity usually necessary without TV recording). The field illumination was filtered by two Calflex heat filters and a Zeiss interference filter (λ_{max} = 554.8 nm, 69%

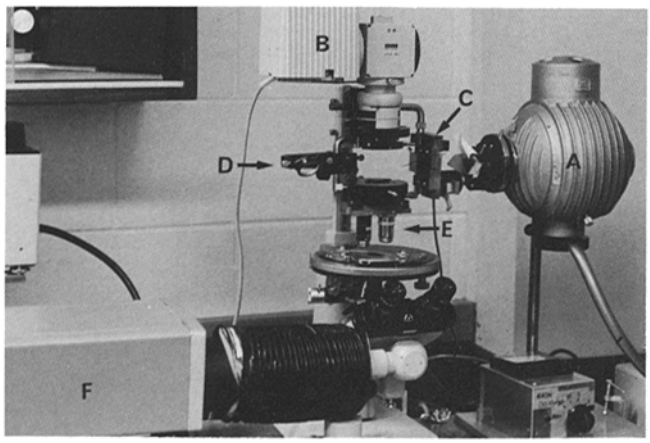

FIGURE 10 The UV-microbeam apparatus. (*A*) 200-W mercury irradiation source with quartz collector. Glass and neutral density filters are suspended in the light path by paper tape to avoid stress cracks during cooling and heating. (*B*) Field illumination source. (*C*) Adjustable rectangular aperture. (*D*) Movable dichroic mirror, now out of the optic axis. (*E*) Quartz × 100 ultrafluar glycerin-immersion and glass × 40 oil immersion objectives in condensor side slider. (*F*) Venus DV-2 intensified television camera. Clothes dryer exhaust duct is used as the flexible light baffle between the microscope and the TV camera.

transmission). The output of the television camera was adjusted using a Ball Brothers waveform monitor and displayed on a 9-in Panasonic 5602 TV monitor in the underscan mode. Experiments were recorded on ¾-in video tape with an NEC 9507 time-lapse video recorder operated in either real time or the 9-h time-lapse mode. The vertical and horizontal linearities of the monitor were adjusted by equilibrating the separation of lines on a stage micrometer at various orientations. Still micrographs were taken of the monitor on Kodak Plus X 35mm film with a Nikon FE using a 55mm Micro Nikkor f 3.5 lens. Images of real time recordings were taken during normal playback of the video recorder. Individual video frames were photographed from time-lapse recordings by double exposing the film to two adjacent interlaced video fields. These negatives were not equivalent to single video frames taken from a real time image in that a video frame represents a $\frac{1}{30}$-s exposure; when recorded in time-lapse mode, a frame now consists of two $\frac{1}{60}$-s fields taken $\frac{2}{15}$ s apart. The magnification on the monitor's screen was × 3,000.

Irradiation Procedure: Mitotic cells were videotaped for a short time prior to irradiation using polarization optics with the matched 40X objectives. When an irradiation was desired, the beam splitter of the microscope was positioned to direct light to the oculars, the 100X quartz objective was slid into the condenser position, and the dichroic mirror rotated into place. The visible image of the irradiation beam (minus the UV component which was filtered out) was focused and centered using the normal condenser controls. The portion of the cell to be irradiated was placed in the beam path using the stage controls. The microscope beam splitter was positioned to direct the image to the television camera, and an image of the beam was recorded. This birefringence image was substantially degraded by the presence of the dichroic mirror and the 100X quartz objective between the analyzer and polarizer. The image could be improved by adjusting the compensator (Zeiss Brace Kohler λ/20) but this required another adjustment after irradiation and was not usually done. The beam splitter was then positioned to prevent light from reaching the camera, and the UV filters (glass) and neutral density filters were removed from the UV-irradiation beam path. The UV-irradiation (duration) was timed with the video recorder's time-date generator, and terminated by returning the filters to the beam path, removing the dichroic mirror, and directing light via the beam splitter back to the television camera. This latter procedure required five seconds or less. If the 40X condenser objective was then slid in place of the 100X objective, another period of <10 s was required after the irradiation. In all cases, the cell was observed and recorded within 15 s of the end of the irradiation. The black-out period on the recording averaged ~1.5 min.

The duration of irradiations varied from 1.5 to 15 s, the period needed to produce a lesion being strongly dependent upon the age of the mercury burner. A power meter (Coherent Inc., Palo Alto, CA) borrowed from the National Bureau of Standards (Boulder, CO), indicated a corrected energy flux of 12 $\mu W/\mu m^2$ at 273-nm wavelength when a 10-s exposure was necessary to generate a lesion in the central spindle. Corrections were made for the transmission of the ultraviolet filter (λ_{max} = 273 nm, 21.5% transmission), the 100X Ultrafluar objective as characterized by Zeiss (transmission, 50%), and the quartz cover slip (transmission, 93.3%). A conveniently available 273-nm filter was used to limit the energy measurements to the portion of the light spectrum damaging to MTs. The visible image of the irradiation aperature could be displaced laterally relative to the UV effect it created in the central spindle if the two were not precisely aligned. This noncorrespondence was best overcome by realigning the lamp housing until the lesion generated in the central spindle became exactly coincident with the visible image of the beam in test cells.

The loss of birefringence from the central spindle of the diatom proved to be a consistent indicator of dosage. This is due to the fact that the spindle somehow integrated the incident energy during the irradiation, and then quite rapidly lost birefringence at the site of irradiation. The production of such a lesion in the MT array was not sensitive to the rapid fluctuations (flickering) characteristic of the 200-W mercury burner. This threshold was sharp enough that a decrease of 1 s from the previously determined lesional exposure would not result in the local loss of birefringence.

Fixations: Cells were immobilized for fixation using the agar-gelatin loop technique of Molé-Bajer and Bajer (31). A 22-mm square quartz cover slip was flamed and coated with 0.1% D,L-polylysine (Sigma Chemical Co., St. Louis, MO). Dividing cells were collected individually and placed on the cover slip. Immediately after the culture medium had been drawn away from the cells, the agar-gelatin (0.4% gelatin and 1% agar) loop was placed over them. This preparation was then inverted on a larger cover slip using silicone grease as a spacer. Each cell was marked with a dot made by a Sharpie pen. The double cover slip preparation was now viewed with a 40X water immersion objective (Zeiss, N.A. 0.75) because of its long working distance. At selected times after irradiation of these cells, 1.5% glutaraldehyde in culture medium (pH 6.8) was drawn between the cover slips by filter paper. Movements of structures such as the cleavage furrow ceased within 5 s of exposure to fixative. After 30 min in glutaraldehyde, the geometry of cells and spots surrounding the irradiated cell was surveyed. The preparation was then removed to a dissecting scope, and the irradiated cell was removed from the agar-gelatin film and placed in a small staining dish. The cell was postfixed with OsO_4 for 10 min, washed, and embedded in a thin layer of 1% agar. The agar block was dehydrated in acetone and flat embedded in Spurr's resin. Thin (75-nm) and thick (0.25-μm and 0.5-μm) serial sections were cut on a Reichert ultramicrotome and collected on slot grids coated with Formvar. Thin sections were viewed at 60 kV on a JEM 100C electron microscope equipped with a goniometer stage. Thick sections were observed on the JEOL 1000 high voltage microscope operated at 1,000 kV.

Ultrastructural Appearance of UV-induced Lesions: When the central spindle was irradiated with an exposure sufficient to generate an area of loss of birefringence, and the cell was then prepared for electron microscopy, the lesion observed in the living cell corresponded to a region in the central spindle devoid of MTs (Fig. 11 *E* and *F*). The size and shape of the lesion viewed in transmission and high voltage transmission electron microscopy appeared to correlate well with the area of reduced birefringence observed and recorded in polarization optics (Fig. 11). In longitudinal sections, the MTs appeared to have been cut sharply at the edge of the lesion. In one case, small dense granules were seen at the lesional ends of MTs distal to the poles. The edges of the lesions often became less even with the passage of time after the irradiation, and this raggedness became more pronounced at the edge proximal to the pole. Occasionally, MT fragments could be seen in the lesion area, but their numbers were small relative to the number of MTs that passed through the area prior to irradiation. In transverse sections of the central spindle, no "C" shaped profiles of MTs were observed at the lesion edges. The pole of the irradiated half spindle contained numerous MTs at oblique angles to the spindle axis. While such MTs are characteristic of the poles in normal cells, MTs of the central spindle pole remaining could also have splayed and thereby contributed to the population of the oblique polar MTs. MTs were morphologically normal after exposure to dosages of UV 1 s less than those which destroyed MTs.

MT lesional dosages of UV light produced areas of lowered staining density in chromosomes (Fig. 6 *G*). These areas coincided positionally, as would be expected, with MT lesions, but only when the cell was fixed immediately after irradiation. Otherwise, the two damaged areas could be displaced relative to each other. Chromosome damage appeared as an expanded "puff" of bleached chromatin, which had not suffered the total loss of organization undergone by irradiated MTs. Such damage was confined to chromosomes nearest the source of irradiation, while others underneath (but in the beam path) were not affected thus. We infer from the preceding observation that an UV dosage slightly greater than the MT-lesional dosage is required to produce morphological damage in chromatin.

The irradiated volume of cytoplasm was predisposed to damage during fixation and dehydration. In cells that were later found in the EM to be badly fixed, vacuoles could be seen to have formed during fixation in the irradiated region viewed in the light microscope. During dehydration, cells were sometimes caught in the air/acetone interface, resulting in repeated cycles of immersion and dessication. The consequent mechanical forces applied to the fixed cell created clear areas in the irradiated portion of the cytoplasm, presumably by rending the

FIGURE 11 An irradiated prometaphase spindle. Time zero is the end of the irradiation. (*A*) −3:27. Birefringence image of a prometaphase spindle. × 2,500. (*B*) 0:00. Diagram of the approximate placement and size of the irradiation beam. The focused aperture is represented by a black rectangle. (*C*) +3:59. The lesion appears as a region of reduced birefringence. The arrows point to the positions of the thin sections shown in *D*, *E*, and *F*. Notice the close correspondence between birefringence adjacent to the lesion in section axis *F* and the MTs apparent in *F*. Fixation was begun as this micrograph was taken. × 2,500. (*D–F*) 0.25-μm sections stained with lead tartrate. *D:* One pair of sister kinetochores are attached to the spindle and appear as chromatin stretched toward opposite poles. Other chromosomes are in prometaphase movement and appear less stretched. The spindle in this section appears to be normal. × 9,700. *E:* The first section in sequence that contained the irradiation lesion. Notice the nearly complete loss of MTs in the lesion; the MTs present here result from a grazing cut of the unirradiated portion of the spindle. × 9,700. *F:* Another section, farther along (*C*), showing again the close correspondence between the birefringence image and the TEM image. × 9,700.

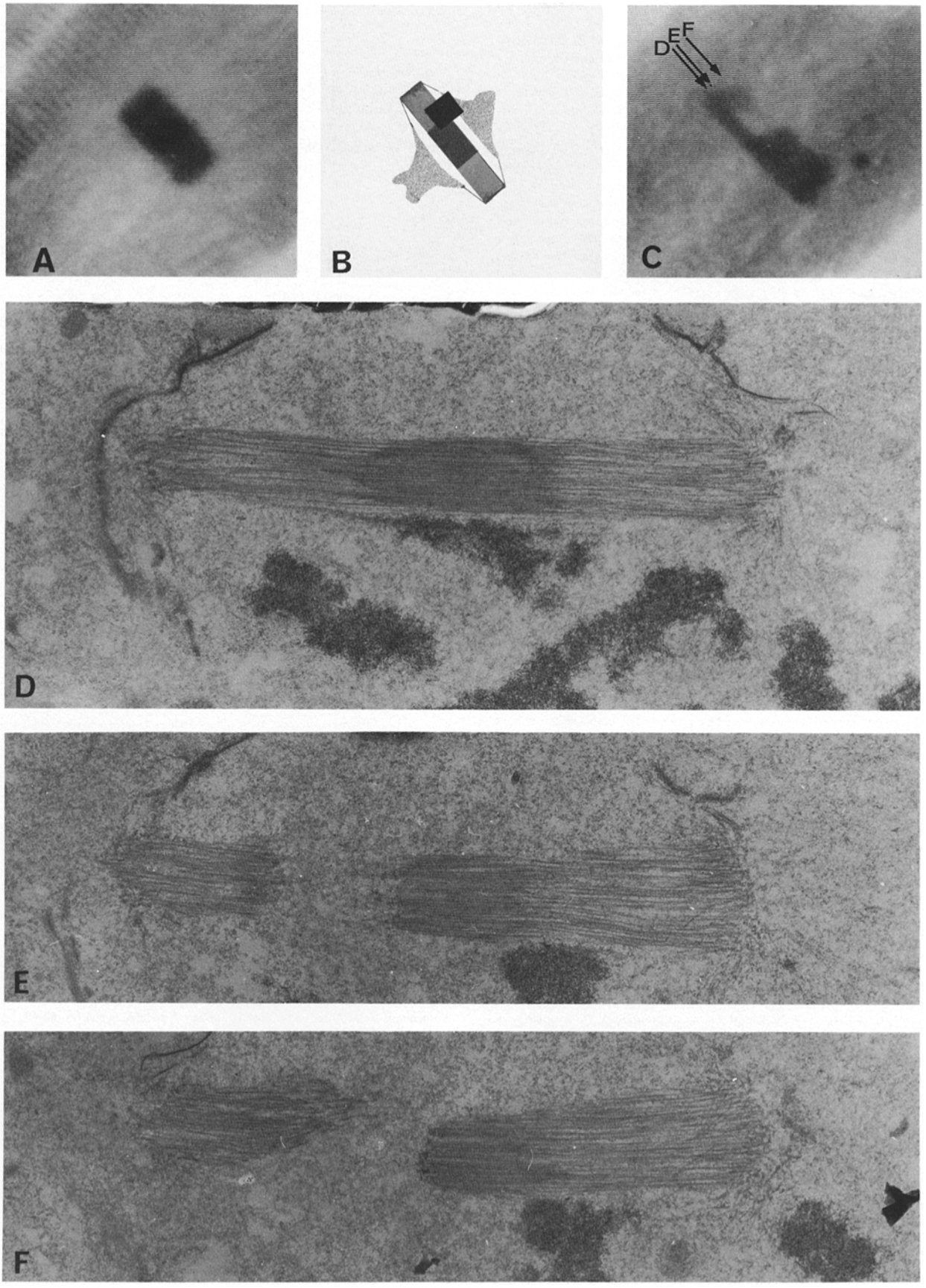
A
B
C
D
E
F
D
E
F

material apart. While the effects visible under the electron microscope were clearly not directly the result of the irradiation, they illustrate a lowered resistance of the cytoplasm generally in irradiated regions, to subsequent mechanical perturbations.

There is a correlation between spot size and the depth of the effected cytoplasmic volume. Micro-slits (8 × 2 μm) disrupted MTs completely through the central spindle along the axis of irradiation. The effects of microsquares (2 × 2 μm) seldom penetrated the full thickness of the central spindle. The result of a small spot lesional-irradiation was a cavity in the central spindle which was bordered on at least three sides by MTs.

Characterization of the UV-Microbeam Lesions: Following well over 200 irradiations with a UV-microbeam, we have shown the diatom central spindle to be an excellent test object for the characterization of UV-microbeam irradiations. This spindle can be used for the precise alignment of the invisible UV beam with the visible component of the same microbeam, and hence align all components to the optical axis. The time required to generate a lesion (a localized loss of birefringence) in the central spindle was so predictable with a given UV source that one can easily use the central spindle as a relative dosimeter for comparing the effects generated on other systems. Following a typical irradiation, we could detect the existence of an affected volume in the cell, when for example, the irradiation generates a clearly defined, localized volume of perturbation in chromosomes on one side of the spindle only. The effect of the beam on chromosomes was different to that on the central spindle, in that the chromosomes closest to the UV-source presumably absorbed enough UV to attenuate the light reaching the apparently unaffected nearby regions (i.e., by shading them). It is also possible that the level of the lesion in the chromatin depends upon the precise focal plane of the UV beam, whereby some chromosomes receive a greater sectional intensity because of beam convergence.

In our experiments the portions of chromosomes affected by the irradiations appeared ultrastructurally expanded and less densely stained. In Fig. 6 *G*, disk-shaped chromosome arm profiles, present elsewhere, are absent in the irradiated region; several are greatly enlarged and dispersed. These observations are morphological confirmation of Perry's (33) deductions from photometric analysis of UV-irradiated chromosomes.

UV-Irradiation of the Spindle: The UV-microbeam produced effects on our central spindle birefringence equivalent to those described by earlier authors on spindle fibres. We did not find a need for through-focus irradiation as described by Bajer (3); the diatom central spindle is thinner (2–3 μm) than the *Haemanthus* spindle. Bajer rejected Forer's (7, 8) interpretations of the effects of irradiation-induced lesions ("Areas of Reduced Birefringence") on the ground that Forer did not use a through focus irradiation and thus may not have completely severed his kinetochore fibers. Our results indicate that an irradiation of the size and shape employed by Forer would almost certainly have severed the MTs of kinetochore fibers in the crane fly spindle, although Forer did not establish this directly. Our assumption is that the spectral characteristics of Forer's irradiation source and ours are similar. Since it required about twice the irradiation dosage to stop a cleavage furrow as to induce a MT lesion in the central spindle, differential susceptibilities of cytoplasmic systems to UV irradiation clearly exist. On this basis, Forer postulated that a second component other than the MTs, could be present and active in the spindle in moving chromosomes. Our present results do not refute this possibility.

The position of the lesion in the central spindle could be shifted laterally (perpendicular to the optic axis) relative to the position of the visible image of the microbeam. In our hands this lateral shift seemed to be an alignment problem in that it could be alleviated by adjusting the lamp housing, aperture position, and condenser alignment. Once aligned in this way, the beam was not shifted laterally regardless of the target (PtK_1, erythrophore, ciliated protozoan, diatom). A small aperature on optic axis should not produce lateral shift problems (8). Forer (7) attributed wavelength dependent lateral shifts in crane fly spermatocytes to dispersion of UV light by cytoplasmic components, including the spindle. He observed greater shifts in the direction perpendicular to the pole to pole axis of the spindle as would be predicted for "the prolate ellipsoid shape of the spindle." The central spindle of *Hantzschia* is a flat band and would not be expected to produce such shape-dependent focus shifts. The direction of the lateral shifts was consistent for any given alignment of the optical components independent of the target; however, we have not yet tested the microbeam with a large prolate ellipsoid spindle such as those in certain cells of the crane fly.

We would like to thank Dr. J. R. McIntosh and Dr. K. R. Porter for equipment loans and kind advice, and Dr. Frank Kowalski and Wyndham Hanaway for their generous counsel. We are also particularly grateful to Dr. James W. Campbell for his encouragement. Preliminary experiments leading to this work were completed in the lab of Dr. A. S. Bajer with the kind help and advice of Dr. Bajer and Dr. J. Molé-Bajer.

This work was supported by grants from National Science Foundation (PCM 80-19707), Public Health Service training grant (NIH GM07413), High Voltage Electron Microscope grant, National Institutes of Health (NIH), Division of Research Resources (RR 00592), NIH (GM 27124), to J. D. Pickett-Heaps, and an equipment donation from Glen Southworth of Colorado Video (Boulder).

Reprint requests should be addressed to Dr. Pickett-Heaps at Molecular, Cellular, and Developmental Biology, Campus Box 347, University of Colorado.

Received for publication 21 May 1982, and in revised form 10 September 1982.

REFERENCES

1. Aist, J. R., and M. W. Berns. 1981. Mechanics of chromosome separation during mitosis in *Fusarium* (fungi imperfecti): new evidence from ultrastructural and laster microbeam experiments. *J. Cell Biol.* 91:446–458.
2. Allenspach, A. L., and L. E. Roth. 1967. Structural variation during mitosis in the chick embryo. *J. Cell Biol.* 33:179–196.
3. Bajer, A. 1972. Influence of UV-microbeam on spindle fine structure and anaphase chromosome movements. *Chromosome Today.* 3:63–69.
4. Belar, K. 1929a. Beitrage zur kausalanalyse der mitose. II. Untersuchungen an den spermatocyten von *Chorthippus* (*Stenobothrus*) *lineatus* Panz. *Roux' Arch.* 118:359–484.
5. Belar, K. 1929. Beitrage zur kausalanalyse der mitose. III. Untersuchungen an den starbfadenhaarzellen und blatmeristemzellen von *Tradescantia virginica. Z. Zellforsch. Mikrosk. Anat.* 10:73–134.
6. Brinkley, B. R., and J. Cartwright, Jr. 1971. Ultrastructural analysis of mitotic spindle elongation in mammalian cells in vitro. *J. Cell Biol.* 50:416–431.
7. Drüner, L. 1895. Studien über ben mechanismus der zellteilung. *Jena Zeitschr.* 29:271–344.
8. Forer, A. 1966. Characterization of the mitotic system and evidence that birefringent spindle fibers neither produce nor transmit force for chromosome movement. *Chromosoma* (*Berl.*). 19:44–98.
9. Forer, A. 1965. Local reduction of spindle fiber birefringence in living *Nephrotoma suturalis* (Loew) spermatocytes induced by ultraviolet microbeam irradiation. *J. Cell Biol.* 25(1, Pt. 2):95*a*. (Abstr.)
10. Gross, F. 1938. The life history of some marine plankton diatoms. *R. Soc. Lond. Phil. Trans. B.* 228:1–48.
11. Heath, B. I., and M. C. Heath. 1976. Ultrastructure of mitosis in the cowpea rust fungus *Uromyces phaseoli* var. vignae. *J. Cell Biol.* 70:592–607.
12. Hughes-Schrader, S. 1947. The pre-metaphase stretch and kinetochore orientation in plasmids. *Chromosoma* (*Berl.*). 3:1–21.
13. Inoué, S. 1964. Organization and function of the mitotic spindle. *In* Primitive Motile Systems in Cell Biology. R. D. Allen and N. Kamiya, editors. Academic Press, Inc., New York.
14. Inoué, S., and H. Sato. 1967. Cell motility by labile association of molecules: the nature of mitotic spindle fibers and their role in chromosome movement. *J. Gen. Physiol.* 50:259–292.
15. Inoué, S., and H. Ritter, Jr. 1975. Dynamics of mitotic spindle organization and function. *In* Molecules and Cell Movement. S. Inoué and R. E. Stephens, editors. Raven Press, New York.
16. Inoué, S., and H. Ritter, Jr. 1978. Mitosis in *Barbulanympha* II. Dynamics of two-stage anaphase, nuclear morphogenesis, and cytokinesis. *J. Cell Biol.* 77:655–684.
17. Izutsu, K. 1961. Effects of ultraviolet microbeam irradiation upon division in grasshopper spermatocytes. II. Results of irradiation during metaphase and anaphase I. *Mie Med. J.* 11(2):213–232.
18. Jenkins, R. A. 1967. Fine structure of division in ciliate protozoa. I. Micronuclear mitosis in *Blepharisma. J. Cell Biol.* 34:463–481.
19. LaFountain, J. R., Jr., and L. A. Davidson. 1980. An analysis of spindle ultrastructure during anaphase of nuclear division in *Tetrahymena. Cell Motility.* 1:41–61.
20. Lauterborn, R. 1896. Untersuchungen uber Bau, Kernteilung and Bewegung der Diatomeen. W. Engelmann, Leipzig.
21. Leslie, R. 1982. Ultraviolet microbeam irradiations of mitotic diatoms. PhD, thesis. University of Oregon, Eugene.
22. McDonald, K. L., J. D. Pickett-Heaps, J. R. McIntosh, and D. H. Tippit. 1977. On the mechanism of anaphase spindle elongation in *Diatoma vulgare. J. Cell Biol.* 74:377–388.
23. McDonald, K. L., M. K. Edwards, and J. R. McIntosh. 1979. Cross-sectional structure of the central mitotic spindle of *Diatoma vulgare.* Evidence for specific interactions between antiparallel microtubules. *J. Cell Biol.* 83:443–461.
24. McIntosh, J. R., P. K. Hepler, and D. G. Van Wie. 1969. Model for mitosis. *Nature* (*Lond.*). 224:659–663.
25. McIntosh, J. R., and S. C. Landis. 1971. The distribution of spindle microtubules during mitosis in cultured human cells. *J. Cell Biol.* 49:468–497.
26. McIntosh, J. R., K. L. McDonald, M. K. Edwards, and B. M. Ross. 1979. Three-dimensional structure of the central mitotic spindle of *Diatoma vulgare. J. Cell Biol.* 83:428–442.
27. McNeill, P. A., and M. W. Berns. 1981. Chromosome behavior after laser microirradiation of a single kinetochore in mitotic PtK_2 cells. *J. Cell Biol.* 88:543–553.
28. Manton, I., K. Kowallik, and H. A. von Stosch. 1970. Observations on the fine structure and development of the spindle at mitosis and meiosis in a marine centric diatom (*Lithodesmium undulatum*). IV. The second meiotic division and conclusion. *J. Cell Sci.* 7:407–443.
29. Margolis, R. L., L. Wilson, and B. I. Kiefer. 1978. Mitotic mechanism based on intrinsic microtubule behavior. *Nature* (*Lond.*). 272:450–452.
30. Mazia, D. 1961. Mitosis and the physiology of cell division. *In* The Cell: Biochemistry, Physiology, Morphology. J. Brachet and A. E. Mirskey, editors. Academic Press, Inc., New York. 77–412.
31. Molé-Bajer, J., and A. Bajer. 1968. Studies of selected endosperm cells with the light and electron microscope the technique. *Cellule.* 67:257–265.
32. Nicklas, R. B. 1963. A quantitative study of chromosomal elasticity and its influence on chromosome movement. *Chromosoma* (*Berl.*). 14:276–295.
33. Perry, R. P. 1957. Changes in the ultraviolet absorption spectrum of parts of living cells

following irradiation with an ultraviolet microbeam. *Exp. Cell Res.* 12:546–559.
34. Pickett-Heaps, J. D., K. McDonald, and D. H. Tippit. 1975. Cell division in the pennate diatom *Diatoma vulgare. Protoplasma.* 86:205–242.
35. Pickett-Heaps, J. D., D. H. Tippit, and J. A. Andreozzi. 1978. Cell division in the pennate diatom *Pinnularia.* II. Later stages in mitosis. *Biol. Cell.* 33:79–84.
36. Pickett-Heaps, J. D., and D. H. Tippit. 1978. The diatom spindle in perspective. *Cell.* 14:455–467.
37. Pickett-Heaps, J. D., D. H. Tippit, and R. J. Leslie, 1980. Light and electron microscopic observations on cell division in two large pennate diatoms, *Hantzschia* and *Nitzschia.* I. Mitosis *in vivo. Eur. J. Cell Biol.* 21:1–11.
38. Pickett-Heaps, J. D., D. H. Tippit, and R. T. Leslie. 1980. Light and electron microscopic observations on cell division in two large pennate diatoms, *Hantzschia* and *Nitzschia.* II. Ultrastructure. *Eur. J. Cell Biol.* 21:12–27.
39. Pickett-Heaps, J. D. 1980. Cell division in the diatom *Pinnularia.* 16mm color, sound film. Cytographics, Boulder, Colorado.
40. Ris, H. 1949. The anaphase movement of chromosomes in the spermatocytes of the grasshopper. *Biol. Bull.* 96:90–106.
41. Roth, L. E., H. J. Wilson, and J. Chakraborty. 1966. Anaphase structure in mitotic cells typified by spindle elongation. *J. Ultrastruct. Res.* 14:460–483.
42. Schmidt, W. J. 1939. Doppelbrechung der kernspindel un zug faser theorie der chromosomen bewugung. *Chromosoma (Berl.).* 1:253–264.
43. Schrader, F. 1953. Mitosis. 2nd edition. Columbia University Press, New York.
44. Smith, F. H. 1935. Anomalous spindles in *Impatiens pallida. Cytologia* 6:165–176.
45. Stephens, R. E. 1965. Analysis of muscle contraction by ultraviolet microbeam disruption of sarcomere structure. *J. Cell Biol.* 25:129–139.
46. Subrahmanyan, R. 1945. On the cell-division and mitosis in some South Indian diatoms. *Proc. Indian Acad. Sci.* 22:331–354.
47. Swann, M. M. 1951. Protoplasmic structure and Meiosis II. The nature and cause of birefringence changes in the sea urchin egg at anaphase. *J. Exp. Biol.* 28:434–441.
48. Taylor, E. W. 1959. Dynamics of spindle formation and its inhibition by chemicals. *J. Biophys. Biochem. Cytol.* 6:193–196.
49. Tippit, D. H., J. D. Pickett-Heaps, and R. Leslie. 1980. Cell division in two large pennate diatoms *Hantzschia* and *Nitzschia.* III. A new proposal for kinetochore function during prometaphase. *J. Cell Biol.* 87:402–416.
50. Tippit, D. H., L. Pillus, and J. D. Pickett-Heaps. 1980b. The organization of spindle microtubules in *Ochromonas danica. J. Cell Biol.* 87:531–545.
51. Tucker, J. B. 1967. Changes in nuclear structure during binary fission in the ciliate *Nassula. J. Cell Sci.* 2:481–498.
52. Zirkle, R. E. 1970. Ultraviolet-microbeam irradiation of newt cell cytoplasm: spindle destruction, false anaphase, and delay of true anaphase. *Rad. Res.* 41:516–537.